HSE
Health & Safety Executive

Investigation of numerical anomalies associated with Transco pipeline upgrade

Prepared by **BOMEL Ltd**
for the Health and Safety Executive 2002

RESEARCH REPORT 021

HSE
Health & Safety Executive

Investigation of numerical anomalies associated with Transco pipeline upgrade

Richard Turner BSc(ENG) C(ENG)
BOMEL Ltd
Ledger House
Forrest Green Road
Fifield, Maidenhead
Berkshire
SL6 2NR

This report concerns an assessment of numerical anomalies found whilst undertaking reliability analyses for a case study as part of a Research Project for the Health and Safety Executive (HSE) Competition of Ideas. The case study was taken from a report produced by the then BG Technology (now Advantica Technologies Limited), and was an example of the application of limit state, reliability and risk-based design techniques to the uprating of onshore pipelines. Probabilistic arguments had been used to demonstrate that the increase in risk as a result of the higher operating pressures in the pipelines was negligible.

The original intention of the case study within the BOMEL project was to use the BG document as an example to demonstrate a practical use of probabilistic methods. It must be clearly stated that the purpose of the case study was not to perform an intensive check of the results obtained.

This report and the work it describes were funded by the HSE. Its contents, including any opinions and/or conclusions expressed, are those of the authors alone and do not necessarily reflect HSE policy.

HSE BOOKS

First published 2002

ISBN 0 7176 2574 5

CONTENTS

EXECUTIVE SUMMARY

This report concerns an assessment of numerical anomalies found whilst undertaking reliability analyses for a case study as part of a Research Project for the HSE Competition of Ideas. The case study was taken from a report produced by the then BG Technology (now Advantica Technologies Limited), and was an example of the application of limit state, reliability and risk-based design techniques to the uprating of onshore pipelines. Probabilistic arguments had been used to demonstrate that the increase in risk as a result of the higher operating pressures in the pipelines was negligible.

The original intention of the case study within the BOMEL project was to use the BG document as an example to demonstrate a practical use of probabilistic methods. It must be clearly stated that the purpose of the case study was not to perform an intensive check of the results obtained.

However, whilst undertaking the BOMEL analysis two interesting anomalies in the results were obtained:

- A step in evaluated probabilities and a change in the governing failure mode from leak to rupture at, or near, the same pressure.

- A 'spike' in probabilities evaluated using the second-order reliability method (SORM) at an interim pressure. Because SORM analysis accounts for the curvature of the failure surface, it usually gives a more accurate answer than first-order linear methods.

These anomalies are of interest because they were unexpected (the BG analysis had been undertaken using numerical integration), and because they are at odds with results based on Monte Carlo simulation. If the sudden increase in failure probability at an interim pressure is "real" it would have serious implications for a Safety Case subsequently built upon the BG example.

The anomalies are also of wider interest because reliability analysis techniques are being used increasingly in a number of areas, often in conjunction with risk-based arguments, to justify or upgrade existing structures or pressure systems.

To investigate the anomalies further in the present study, the original problem has been simplified. Only two random variables have been used, but the essential elements of the problem, trends in failure probabilities, etc, and the anomalies have been retained.

This investigation into the anomalies has shown that the evaluated reliabilities are partly a result of analysis methodologies (FORM/SORM) used in this report and not as a result of a "real" aberration in pipeline

behaviour under pressure . The approach adopted by BG Advantica was not subject to the limitations of these methods and their results did not display the anomalous behaviour. It is emphasised therefore, that the conclusions have no relevance to the BG Advantica work but are provided for guidance to Users less familiar with these techniques.

The particular circumstances that have lead to the anomaly in the SORM results, whilst interesting, are believed to be unusual in practice. The particular failure function and probability distribution modelling lead to circumstances where the standard second-order reliability methods usually used in general-purpose software breakdown. In this case, it is evidenced by the very large second-order correction terms that are applied to the FORM results at particular pressures.

The case study analysis was undertaken using commercial reliability software, and this work has shown that when undertaking reliability analysis of even a simple problem it is very important to have a thorough understanding of the theory, the software, convergence tolerances, and the various analysis options available.

This investigation has also shown that when undertaking a reliability analysis of this sort it is important to undertake parameter studies, sensitivity studies, and to check the evaluation of the failure probability using at least two alternative methods. These points were recommended in the final report for the Competition for Ideas project.

1. INTRODUCTION

1.1 INTRODUCTION

This report concerns an assessment of numerical anomalies found whilst undertaking reliability analyses for a case study as part of a Research Project for the HSE Competition of Ideas. The title of the Research Project undertaken by BOMEL was 'Probabilistic Methods – uses and abuses in structural integrity' [1], and the particular case study in question was taken from a report produced by the then BG Technology (now Advantica Technologies Limited) supplied to BOMEL by HSE [2].

The BG document describes an example of the application of limit state, reliability and risk-based design techniques to the uprating of onshore pipelines. The BG work stemmed specifically from a study of the feasibility of uprating approximately 400 km of high-pressure gas transmission pipelines. The pipelines under consideration are 914.4mm x 12.7mm wall thickness, API 5L grade X60 material. At the time of the study the pipelines were operated at a design pressure of 70 barg (7 MPa) and the proposal was to increase the design pressure to 85 barg (8.5 MPa). This would involve stepping outside current design rules by increasing the maximum design factor from the current allowable of 0.72 to a value of 0.78. Probabilistic arguments had been used to demonstrate that the increase in risk as a result of the higher operating pressures was negligible.

The original intention of the case study within the BOMEL project was to use the BG document as an example to demonstrate a practical use of probabilistic methods. It must be clearly stated that the purpose of the case study was not to perform an intensive check of the results obtained.

However, whilst undertaking the analysis two interesting anomalies in the results were obtained:

- A step in evaluated probabilities and a change in the governing failure mode from leak to rupture at, or near, the same pressure.
- A 'spike' in probabilities evaluated using the second-order reliability method (SORM) at an interim pressure. Because SORM analysis accounts for the curvature of the failure surface, it usually gives a more accurate answer than first-order linear methods.

The anomalies are illustrated in Figures 1.1 and 1.2, which are copied from the BOMEL report [1].

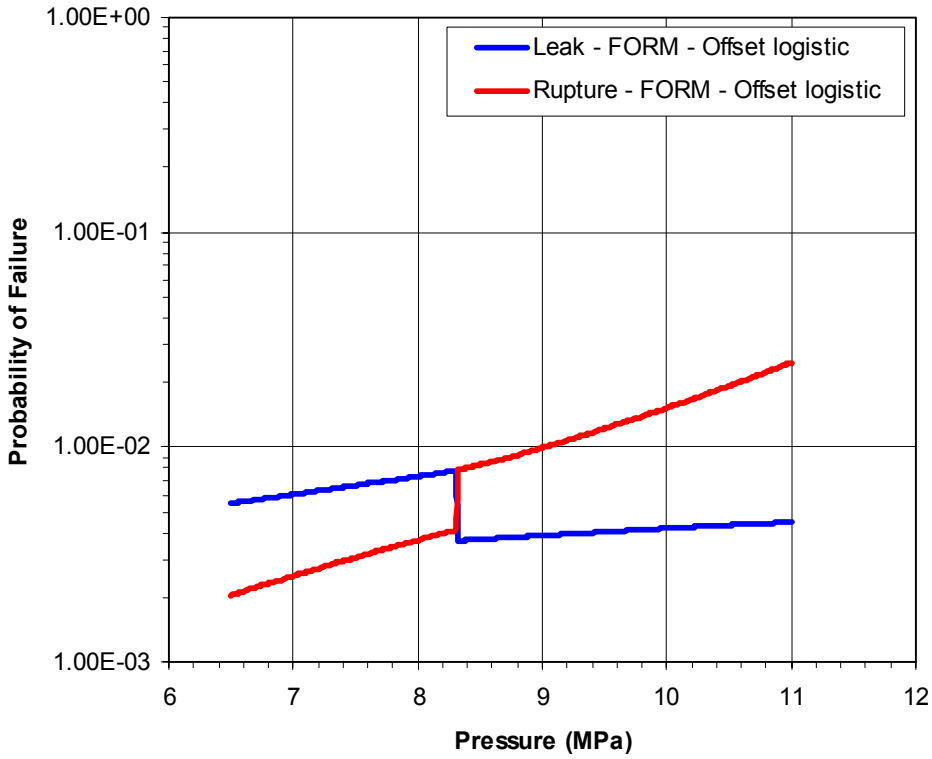

Figure 1.1 Case Study Results – FORM anomaly

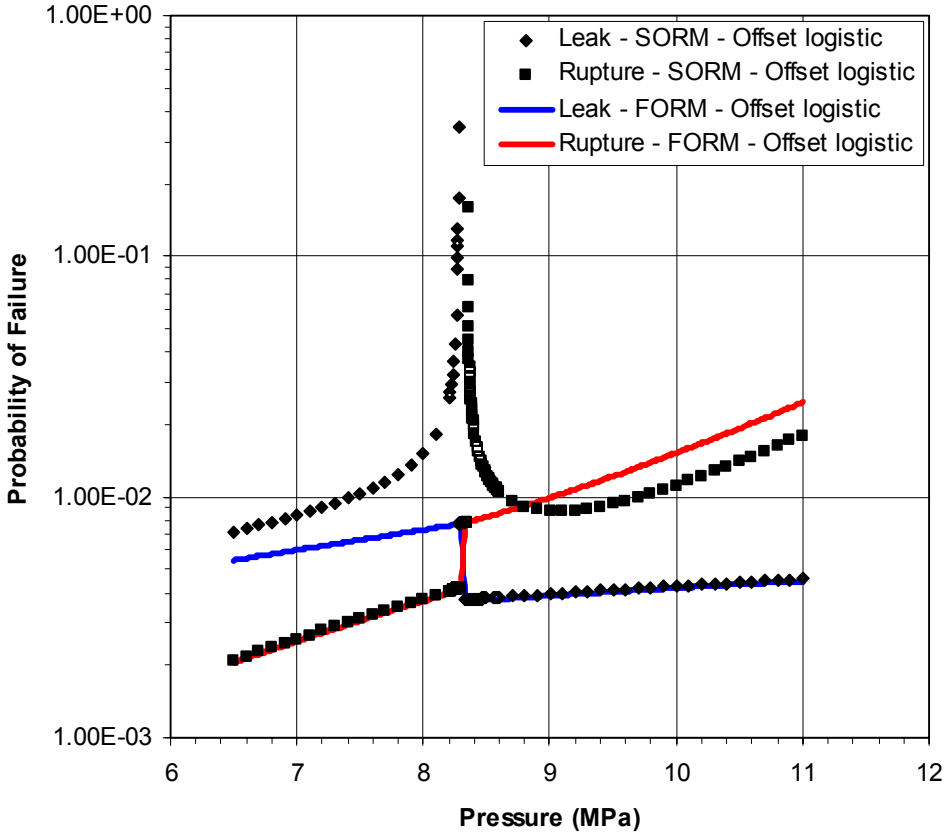

Figure 1.2 Case Study Results – SORM anomaly

These anomalies are of interest because they were unexpected (the BG analysis had been undertaken using numerical integration), and because they are at odds with results based on Monte Carlo simulation. If the sudden increase in failure probability at an interim pressure is "real" it would have serious implications for a Safety Case subsequently built upon the BG example.

1.2 SCOPE OF WORK

There are a number of secondary factors that may influence and complicate the original problem, including the possibility of pipe denting and the use of complex probability distribution types. The first step of this more detailed investigation was to simplify the problem as far as possible whilst still maintaining the essential elements of the 'spike' in probability for the SORM results and the step in probability results between failure governed by leak and rupture.

The next task was to investigate the step in evaluated reliabilities and the change in the governing failure modes.

The final task was to investigate the reasons for the anomalous findings in the SORM results.

2. PROBABILISTIC MODEL

2.1 SUMMARY

The example concerns the evaluation of the probability of failure of a pressurised pipe due to external interference. Failure is defined as a loss of containment leading to a release of gas, and this may occur as the result of a leak or a rupture. The consequences that may result from a rupture may be more severe than a leak, and so the probability of failure as a result of a rupture and probability of failure as a result of a leak are both of interest. (It should be noted that the pipe may fail as a result of other hazards, such as stress corrosion cracking, hydrogen-induced cracking, internal and external corrosion and construction defects, but these are not considered here).

This section describes the failure modes and functions, the basic variables, and how the problem has been simplified to investigate the anomalies.

2.2 FAILURE MODES AND FUNCTIONS

2.2.1 Failure Modes

The failure modes considered in the case study stemmed from damage due to external interference. Such external interference may result in either a puncture of the pipe wall or in a dent and / or gouge in the pipe wall. The metal loss, and associated stress concentration and intensification, corresponding to a gouge may result in failure of the pipe wall ligament under internal pressure loading.

The case study concentrated on the gouging and / or denting failure mechanism. Gouge / dent defects are characterised by gouge depth and length, and dent depth (which may be zero in a situation where a gouge occurs without a dent). However, the case study analyses showed that, the variables and probability distributions defining dent depth were shown not to influence the evaluated failure probabilities or anomalies in question (see below), thus denting may be eliminated from further consideration here.

Three consequences may arise from the presence of a gouge defect:

- The gouge depth may be of a sufficient magnitude to grow rapidly to a through thickness defect, whereupon a leak will occur.
- If, in addition to this, the length of the gouge exceeds a critical value then rupture will occur.
- Neither leak nor rupture will occur if the gouge depth and length are less than their respective critical values (although there may be fatigue implications, not considered here, resulting from pressure cycling).

It is evident that to cover the domain of the problem two failure functions are required, relating to:

- Critical gouge depth
- Critical gouge length.

The failure domain can be defined as follows:

- If the gouge depth, a, is greater than the critical gouge depth, a_c, loss of containment occurs by either a leak or a rupture, i.e. $\{a \geq a_c\}$.

- A leak occurs if the gouge depth is greater than the critical gouge depth AND the gouge length, L, is less than the critical length, L_c, i.e. $\{a \geq a_c \cap L < L_c\}$.

- A rupture occurs if the gouge depth is greater than the critical gouge depth AND the gouge length is greater than the critical length, i.e. $\{a \geq a_c \cap L \geq L_c\}$.

The modelling of critical gouge depth and critical gouge length are dealt with in the following two subsections.

2.2.2 Critical Gouge Depth

Gouges situated in dents are assessed using a fracture mechanics approach that assumes that a gouge behaves as a crack. The failure function is given by:

$$K_r = S_r \left[\frac{8}{\pi^2} \ln\left\{ \sec\left(\frac{\pi}{2} S_r \right) \right\} \right]^{-1/2}$$

where K_r and S_r are dimensionless material toughness and stress ratio parameters, respectively. Their compositions are explained below. Before that, it is more convenient to rearrange this function and note that the depth of a gouge exceeds a critical value if:

$$\cos\left(\frac{\pi}{2} S_r \right) - \exp\left[-\frac{\pi^2}{8} . \frac{S_r^2}{K_r^2} \right] < 0$$

K_r and S_r are given by:

$$K_r = \frac{\left[\sigma_m Y_m(a,w) + \sigma_b Y_b(a,w) \right] \sqrt{\pi a}}{K_{IC}}$$

$$S_r = \frac{\sigma_m \left(1 - \frac{a}{Mw} \right)}{\sigma_f \left(1 - \frac{a}{w} \right)}$$

In these equations σ_m is a membrane stress given by:

$$\sigma_m = \sigma_h\left(1 - 1.8\frac{D}{2R}\right)$$

σ_b is a bending stress, present due to dent of depth D, given by:

$$\sigma_b = 10.2\sigma_h\frac{D}{2w}$$

and σ_h is the hoop stress in the pipe wall, given by:

$$\sigma_h = \frac{PR}{w}$$

Since the dent depth D is assumed to be zero here, $\sigma_m = \sigma_h$, and $\sigma_b = 0$.

The gouge depth is denoted by a, and R and w denote the pipe radius and wall thickness, respectively.

The quantities Y_m and Y_b are functions of gouge depth and pipe wall thickness, and are normalised stress intensity factors for an edge-cracked strip in tension and bending, respectively. (The expression for Y_b is given for completeness, but is not used since $\sigma_b = 0$). They are given by:

$$Y_m = 1.12 - 0.23\left(\frac{a}{w}\right) + 10.6\left(\frac{a}{w}\right)^2 - 21.7\left(\frac{a}{w}\right)^3 + 30.4\left(\frac{a}{w}\right)^4$$

$$Y_b = 1.12 - 1.39\left(\frac{a}{w}\right) + 7.3\left(\frac{a}{w}\right)^2 - 13.0\left(\frac{a}{w}\right)^3 + 14.0\left(\frac{a}{w}\right)^4$$

The Folias factor M is given by:

$$M = \left[1 + 0.26\frac{L^2}{Rw}\right]^{1/2}$$

where L is the gouge length. The material flow stress σ_f is expressed in terms of the material yield and ultimate strengths of σ_y and σ_u as:

$$\sigma_f = \alpha\left(\sigma_y + \sigma_u\right)$$

where α is a flow stress parameter.

The material fracture toughness, K_{IC}, is found from the Charpy energy using the following correlation:

$$K_{IC} = \left(\frac{EC_{v0}}{A}\right)^{1/2}\left(\frac{C_v}{C_{v0}}\right)^{1/2b}$$

where E is Young's modulus of the material, A is the area of the Charpy test specimen, b is a dimensionless parameter, and C_{v0} is a reference Charpy energy.

2.2.3 Critical Gouge Length

If the depth of a gouge exceeds a critical value, then a through-wall defect results. If the length of such a through-wall defect exceeds a critical value, then rupture will occur. Such a situation obtains if:

$$\sqrt{\left[\left(\frac{\sigma_h}{1.150\sigma_y}\right)^{-2} - 1\right].\frac{Rw}{0.4}} - L < 0$$

The terms within the square-root sign can be interpreted as representing a critical length L_c.

It is worthwhile noting that, whilst the failure function for gouge depth incorporates both plastic collapse and fracture (i.e. incorporates both flow stress and fracture toughness), the failure function for gouge length appears to only involve collapse.

2.3 INPUT PARAMETERS AND DISTRIBUTIONS

2.3.1 List of Parameters and Distribution Specification

The parameters used as inputs to the failure functions in the BOMEL case study [1] are summarised in Table 2.1. All variables were assumed to be independently distributed, i.e. uncorrelated.

Figure 2.1 shows the sensitivities and elasticities for the basic variables that were obtained in the case study at a pressure of 7.0 and 9.0 MPa. The sensitivities and elasticities measure the rate of change of the reliability index (and therefore also of the failure probability) with respect to the mean or standard deviation of the variable concerned. (Elasticities for the standard deviation of a variable are almost always negative because an increase in standard deviation usually decreases the reliability index (increases the probability of failure)).

Variable	Description	Units	Type	Value / Parameters	
R	Pipe outside radius	mm	Deterministic	457.2	
w	Pipe wall thickness	mm	Normal distribution	μ = 12.8, Φ = 0.3	
α	Flow stress parameter	-	Deterministic	0.5	
σ_y	Pipe material yield strength	MPa	Lognormal distribution	μ = 445.9, σ = 12.8	
σ_u	Pipe material ultimate strength	MPa	Normal distribution	: = 593.4, σ = 14.5	
E	Pipe material Young's modulus	MPa	Deterministic	207 x 10^3	
C_v	Charpy energy	mJ	Lognormal distribution	: = 55200, Φ = 11100	
C_{v0}	Reference Charpy energy	mJ	Deterministic	112300	
A	Charpy test specimen cross-section area	mm^2	Deterministic	53.55	
b	Charpy energy correlation parameter	-	Deterministic	0.4950	
a	Gouge depth	mm	Weibull distribution	α = 0.73 β = 0.98	
L	Gouge length	mm	Offset logistic distribution	$\forall_L$, $\exists_L$, γ_L see below	
D	Dent depth	mm	Bespoke distribution	α_D, β_D, D_D see below	
α_L	Parameters used in statistical distribution for gouge length L (see below)	-	Deterministic	0.043	
β_L		mm	Deterministic	24.84	
γ_L		mm	Deterministic	30.13	
N		-	Normal distribution	μ = 0, σ = 1.0	
α_D	Parameters used in statistical distribution for dent depth D (see [1])	-	Deterministic	0.9	0.9
β_D		mm	Deterministic	4.91	4.49
D_D		-	Normal distribution	μ = 0, σ = 1.0	
P	Operating pressure	MPa	Deterministic	7.0 (70 barg)	9.0 (90 barg)

Table 2.1 Parameters used as Inputs to Failure Functions in the Case Study (baseline analyses)

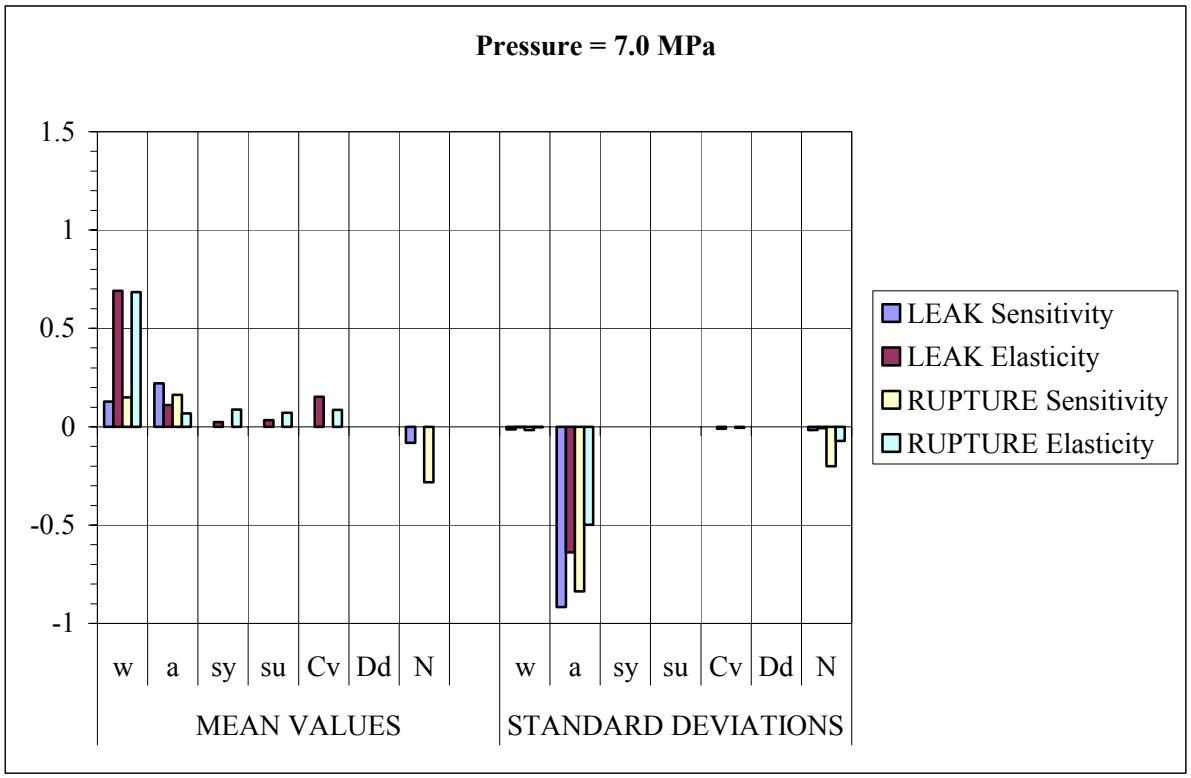

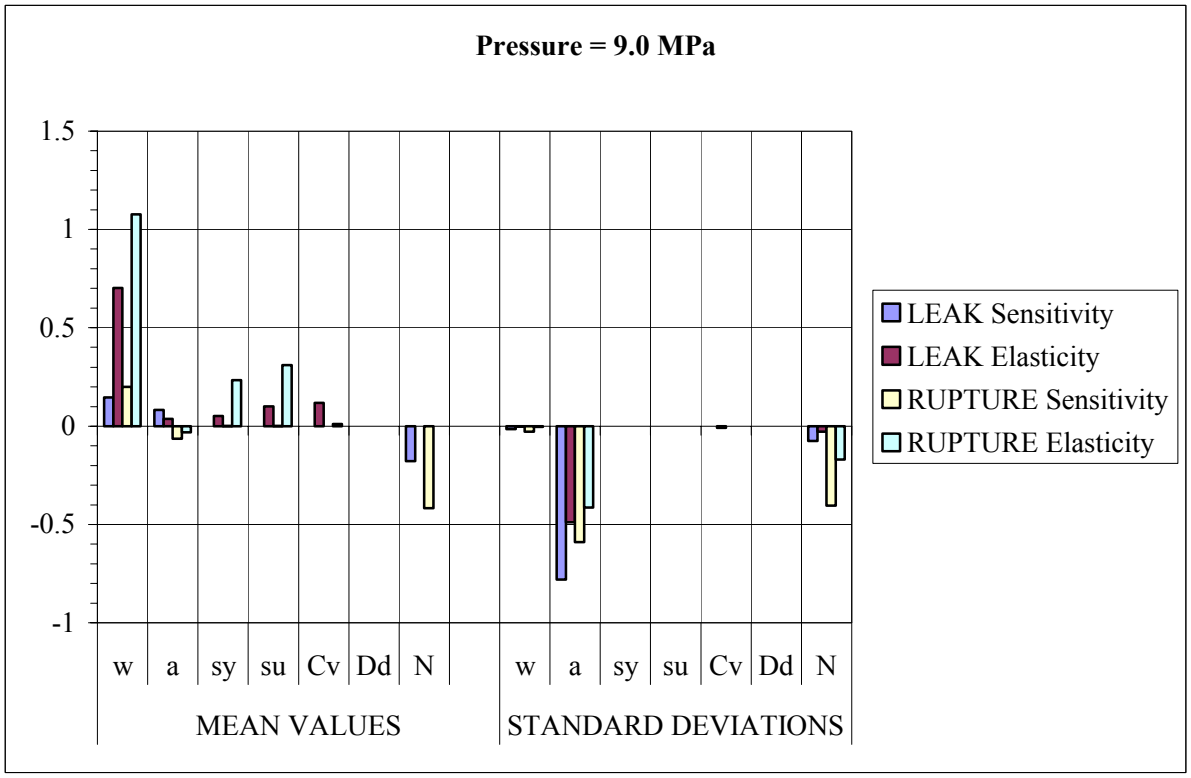

Figure 2.1 Baseline Analyses of 7 and 9 MPa Internal Pressures. Sensitivities and Elasticities of Means and Standard Deviations of Basic Variables

Whilst the mean value of wall thickness, w, has a significant influence on reliability, reliability is not very sensitive to its standard deviation. Dent depth has no influence on reliability at the most likely failure point, and has no influence on the anomalies identified in [1]. As discussed above, it may be eliminated here.

The most sensitive variable is gouge depth, a, followed by gouge length (modelled using the standard normal variable, N). The effect of the uncertainty in the other variables is low. Therefore, all of the other variables, including wall thickness, may be treated as deterministic; the mean value has been used. This significantly simplifies the problem, because there are only two basic variables gouge depth and gouge length. Table 2.2 summarises the parameters used in the simplified model.

Variable	**Description**	**Units**	**Type**	**Value / Parameters**	
R	Pipe outside radius	mm	Deterministic	457.2	
w	Pipe wall thickness	mm	Deterministic	12.8	
α	Flow stress parameter	-	Deterministic	0.5	
σ_y	Pipe material yield strength	MPa	Deterministic	445.9	
σ_u	Pipe material ultimate strength	MPa	Deterministic	593.4	
E	Pipe material Young's modulus	MPa	Deterministic	207×10^3	
C_v	Charpy energy	mJ	Deterministic	55200	
C_{v0}	Reference Charpy energy	mJ	Deterministic	112300	
A	Charpy test specimen cross-section area	mm^2	Deterministic	53.55	
b	Charpy energy correlation parameter	-	Deterministic	0.4950	
a	Gouge depth	mm	Weibull distribution	$\alpha = 0.73$ $\beta = 0.98$	
L	Gouge length	mm	Offset logistic distribution	α_L, β_L, γ_L see below	
D	Dent depth	mm	Deterministic	0.0	
α_L	Parameters used in statistical distribution for gouge length L (see below)	-	Deterministic	0.043	
β_L		mm	Deterministic	24.84	
γ_L		mm	Deterministic	30.13	
N		-	Normal distribution	$\mu = 0$, $\sigma = 1.0$	
P	Operating pressure	MPa	Deterministic	7.0 (70 barg)	9.0 (90 barg)

Table 2.2 Simplified Parameters used as Inputs to Failure Functions (baseline analyses)

Whilst the numerical values of the probabilities evaluated from this simplified modelling are slightly different from those evaluated using the complete modelling, the trends in probability with pressure and the essential elements of the numerical anomalies in question are retained, as shown in Section 3.

Gouge Length – Offset Logistic Distribution

The cumulative distribution function for the offset logistic probability density function is written as:

$$X = \frac{1}{1 + \exp\left(\gamma_L - \beta_L x^{\alpha_L}\right)}$$

The inverse of this is:

$$x = \left[\frac{1}{\beta_L}\left\{\gamma_L - \ln\left(\frac{1-X}{X}\right)\right\}\right]^{\frac{1}{\alpha_L}}$$

Thus gouge length may be modelled using the standard normal variable N, as follows:

$$L = \left[\frac{1}{\beta_L}\left\{\gamma_L - \ln\left(\frac{1-\Phi(N)}{\Phi(N)}\right)\right\}\right]^{1/\alpha_L}$$

with the condition that L = 0 if N <1. The function Φ is the standard normal cumulative distribution.

3. RELIABILITY RESULTS AND DISCUSSION

3.1 SUMMARY

This section presents further reliability results undertaken to investigate the numerical anomalies, and discusses the underlying causes of them.

As for the case study work, the reliability analysis was undertaken using the commercial software package SYSREL [3].

3.2 STEP IN RELIABILITY RESULTS

The first anomaly is most evident in the FORM results, which shows:

- A switchover of the failure probabilities: at low pressures the higher probability is associated with leak and the lower with rupture; the converse is true at high pressures.
- Steps in the graphs where the leak and rupture probabilities jump down and up, respectively.

3.2.1 Switchover in governing failure mode

The switchover in the dominant failure mode is a phenomena of the modelling and assumptions of the problem being analysed, and can be demonstrated using Monte Carlo analysis.

Figure 3.1 shows the results of analysis using adaptive sampling; enough trials have been taken in the Monte Carlo analysis such that the results tend to the exact failure probability defined by the numerical modelling of the failure surfaces and basic variable probability distributions. (The Monte Carlo results are also shown in Figures 3.12 to 3.14 where they are compared with FORM and SORM results.) The Monte Carlo results suggest that the switchover in governing failure mode occurs at a pressure of around 8.45 MPa in this example.

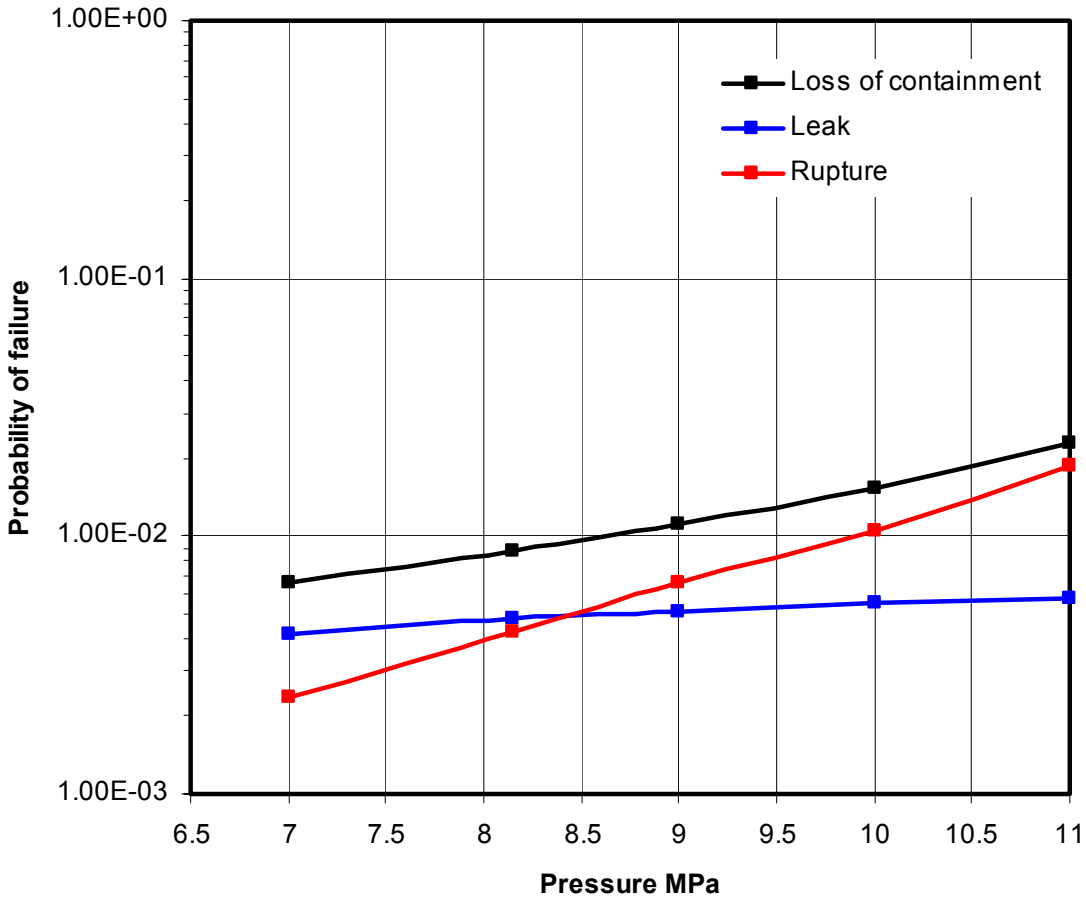

Figure 3.1 Monte Carlo analysis results for leak and rupture

3.2.2 Step in failure probability

As suggested in the BOMEL case study report [1], further investigation has shown that the steps in the probabilities evaluated by FORM occur as a result of the use of a default option in the SYSREL software. The option is to select/deselect inactive constraints. In SYSREL, the default is to deselect or switch off the evaluation of inactive constraints.

In reliability theory, a failure boundary or failure surface is often referred to as a constraint. An inactive constraint is the failure surface of a mode or failure function in the reliability analysis problem that does not pass through the beta-point, i.e. the point closest to the origin (or the point with the highest probability density in the failure region).

In order to understand the significance of inactive constraints it is necessary to understand how first- and second-order reliability methods approximate the failure region. Initially, FORM/SORM and the significance of the beta-point for a single failure event is outlined, and then methods for approximating the intersection of probabilities for two failure events is discussed. Then the particular results for the case study are presented.

3.2.2.1 Single failure event

For simple problems involving a single failure event or failure function, first- and second-order reliability methods are based on iterating to find the beta-point, and then approximating the failure region, or rather the boundary of the failure region, using a surface based on the gradient and curvature information at this point. In most cases this gives a sufficiently accurate estimate of the probability of failure. However, the accuracy of the estimate clearly depends on how well the fitted surface approximates the failure surface, particularly in the region around the beta-point.

3.2.2.2 Intersection of probabilities for two failure events

Now consider the evaluation of the probability of the intersection of two failure events. It is possible to obtain a first-order estimate by finding the beta-point for each failure surface, fitting a hyperplane to the failure surface at each point, and evaluating the intersection of the two hyperplanes analytically. In SYSREL, this is termed crude FORM. This is illustrated in Figure 3.2 on the right hand side.

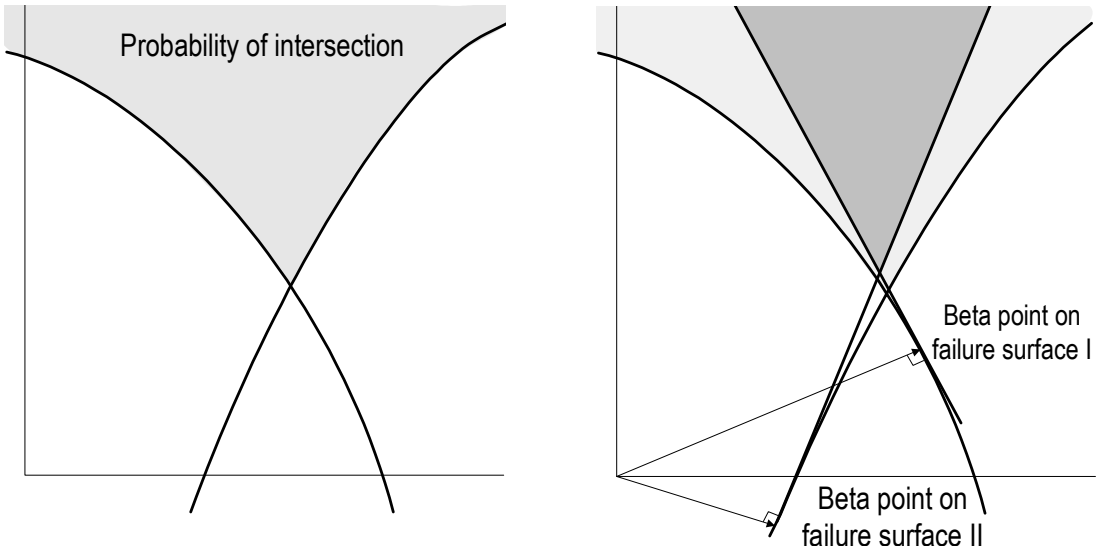

Figure 3.2 Schematic intersection of events and first-order estimate based on hyperplanes

A better first-order estimate can be finding the point of intersection of the two failure surfaces, and utilising the gradient information of both of the failure surfaces at this joint beta-point. This is the method used in SYSREL, and is illustrated in Figure 3.3.

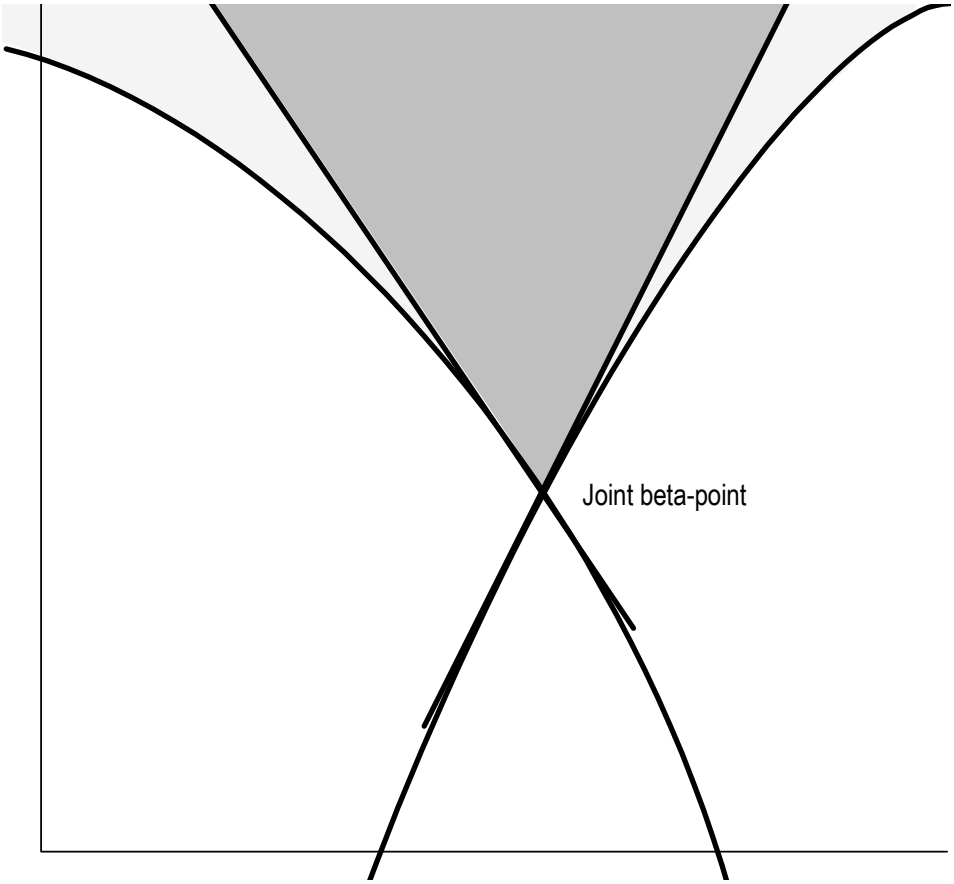

Figure 3.3 First-order estimate based on joint-beta point

However, if the joint beta-point is not the closest point to the origin in the failure region, the default method for the SYSREL program will iterate to find the closest point and estimate the failure probability by fitting a hyperplane at this point, as illustrated in Figure 3.4 by the hatched area. The other failure function is therefore inactive, i.e. an inactive constraint.

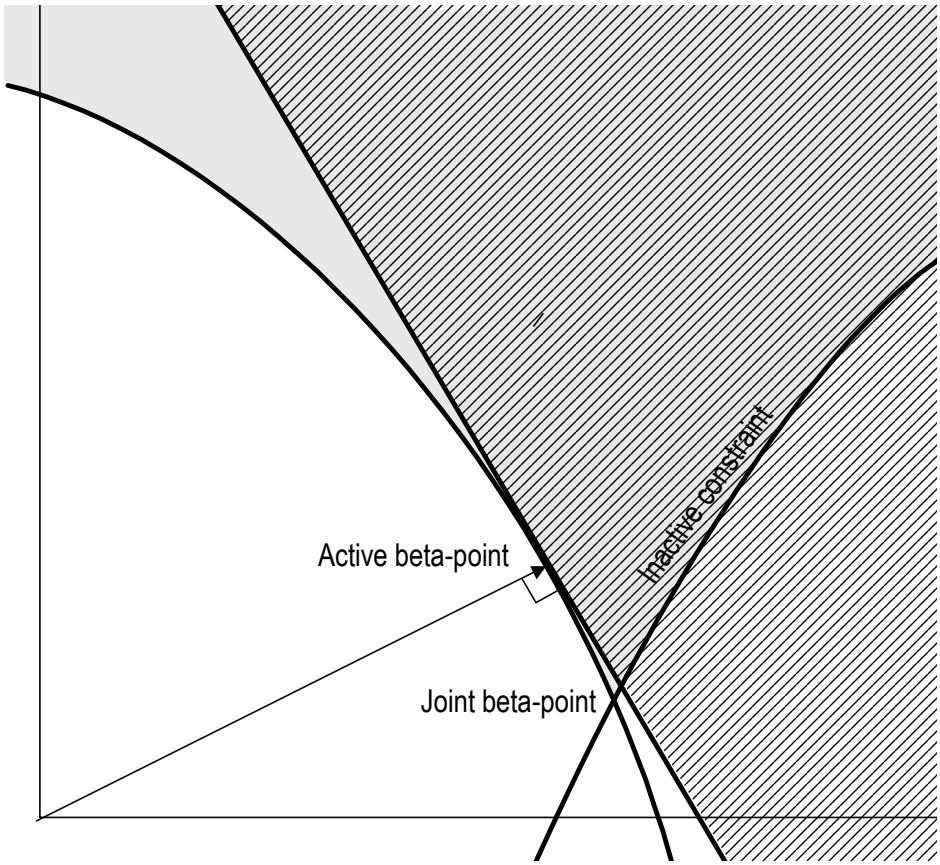

Figure 3.4 Illustration of inactive constraint

In many cases this gives a sufficiently accurate estimate of the failure probability. However, a better estimate can be found by seeking out the joint beta-point with the inactive constraint as well as the active beta-point. Clearly, this involves more numerical effort, and in a complex problem involving a number of basic variables and active and inactive constraints it may involve considerable numerical effort. Thus, the default option in SYSREL is to skip the inactive constraints.

When the default option is chosen to skip inactive constraints, jumps can occur in the evaluated failure probability when undertaking parameter studies, e.g. increasing the pressure in this case study example since, depending where the joint beta-point is, the failure probability may be evaluated as illustrated in Figure 3.3 or Figure 3.4. When the joint beta-point coincides with the closest point to the origin the failure probability that will be evaluated is illustrated in Figure 3.5 – the failure probability may either be evaluated using the dark shaded area or the hatched area depending on whether the second constraint is active or not within the numerical tolerance of the program.

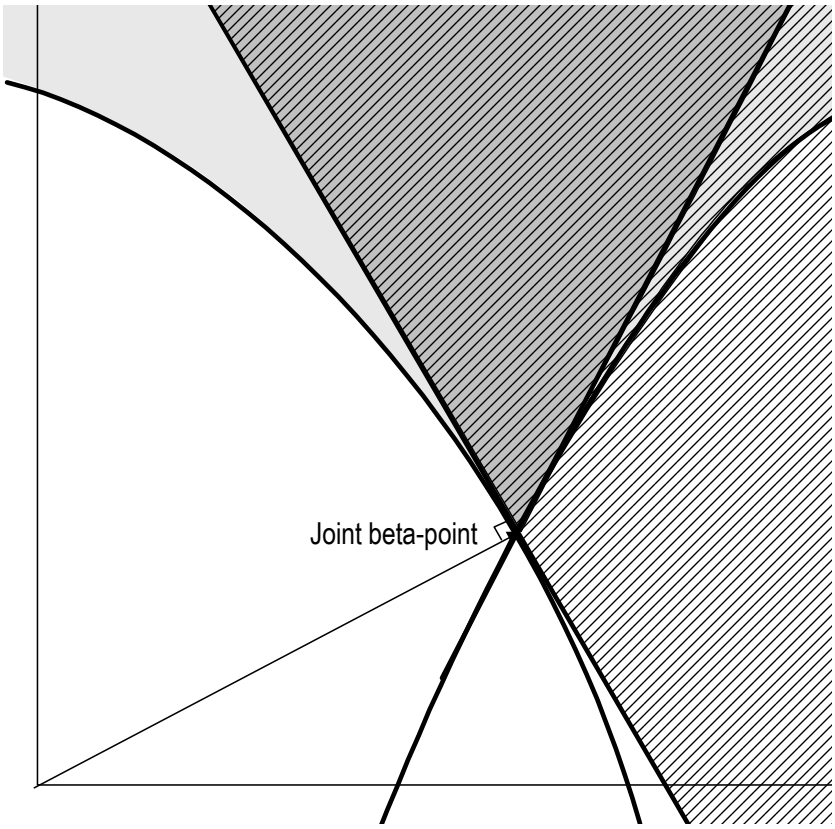

Figure 3.5 Illustration of switching in failure region due to active/inactive constraint

3.2.2.3 FORM results for active and inactive constraints

Now consider first-order reliability analysis of the case study example. First-order results for the case study are illustrated in Figure 3.6, and are discussed in detail below. Results with the evaluation of the inactive constraints skipped are shown with square symbols, and results including the evaluation of inactive constraints are shown with a bold line.

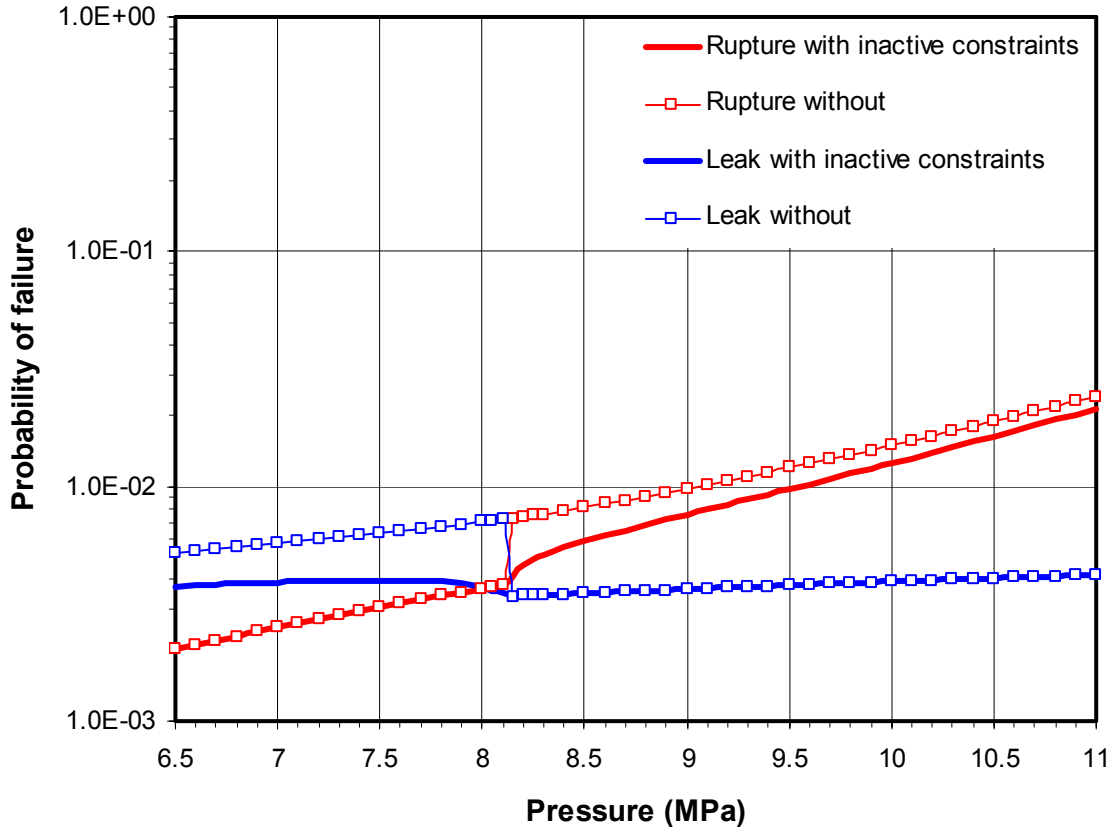

Figure 3.6 FORM results based on active and inactive constraints

For a leak, the failure domain can be defined by as follows:

- if the gouge depth is greater than the critical gouge depth AND the gouge length, L, is less than the critical length, L_c, i.e. $\{a \geq a_c \cap L < L_c\}$.

The results for the probability of a leak are shown in blue in Figure 3.6. Below a pressure of around 8.15 MPa, where the step occurs in this case, the governing beta-point (i.e. the closest point to the origin) is only associated with the first criterion (i.e. gouge depth ≥ critical), and the second criteria represents an inactive constraint (e.g. illustrated schematically by Figure 3.4). As pressure is increased to the "step" value, the second criterion (i.e. gouge length ≤ critical) is activated. At pressures in excess of this, both criteria remain active and the beta point continues to be associated with the critical gouge length (e.g. illustrated schematically by Figure 3.3).

When this is evaluated using first-order reliability with the inactive constraints option switched ***off*** there is a step in the evaluated failure probability at a pressure of around 8.15 MPa, in this case. When evaluated with the inactive constraints option switched ***on*** there is a discontinuity in the gradient of the evaluated failure probability at a pressure of around 8.15 MPa, but no step, and for pressures below 8.15 MPa the failure probability for a leak evaluated using the inactive constraint is smaller and is a much better estimate of the 'true' probability of failure.

Similarly, for a rupture, the failure domain can be defined as follows:

- if the gouge depth is greater than the critical gouge depth AND the gouge length is greater than the critical length, i.e. $\{a \geq a_c \cap L \geq L_c\}$.

At low pressures both criteria (gouge length ≥ critical) are activated, and the beta-point is associated with the critical length. As pressure increases, the second criterion becomes de-activated, and the governing beta-point is only associated with the critical gouge depth.

Again, with the inactive constraints option switched ***off*** there is a step in the evaluated failure probability at a pressure of around 8.15 MPa, and with the inactive constraints option switched ***on*** there is a discontinuity in the gradient of the evaluated failure probability. For pressures above 8.15 MPa, the failure probability for a rupture evaluated using the inactive constraint is smaller and is a much better estimate of the 'true' probability of failure.

The probability of a loss of containment, due to a leak OR a rupture, can be evaluated as the union of the probabilities for the two events, i.e.

$$P\left\{\{a \geq a_c \cap L < L_c\} \bigcup \{a \geq a_c \cap L \geq L_c\}\right\}$$

The first-order reliability results are shown in Figure 3.7. The failure probability for a leak is shown by the solid blue line, for a rupture by the solid red line, and for the union of the probabilities evaluated by SYSREL by the broken black line.

However, since $P\{L < L_c\} = 1 - P\{L \geq L_c\}$ it can be shown that

$$P\left\{\{a \geq a_c \cap L < L_c\} \bigcup \{a \geq a_c \cap L \geq L_c\}\right\} = P\{a \geq a_c\}$$

First-order results for this case, evaluated using the gouge depth criterion only, are shown by the solid black line in Figure 3.7.

In principle, the dashed line and the solid black line in Figure 3.7 should coincide. However, both are acceptable first-order estimates of the combined probability of failure due to loss of containment (by either leak or rupture).

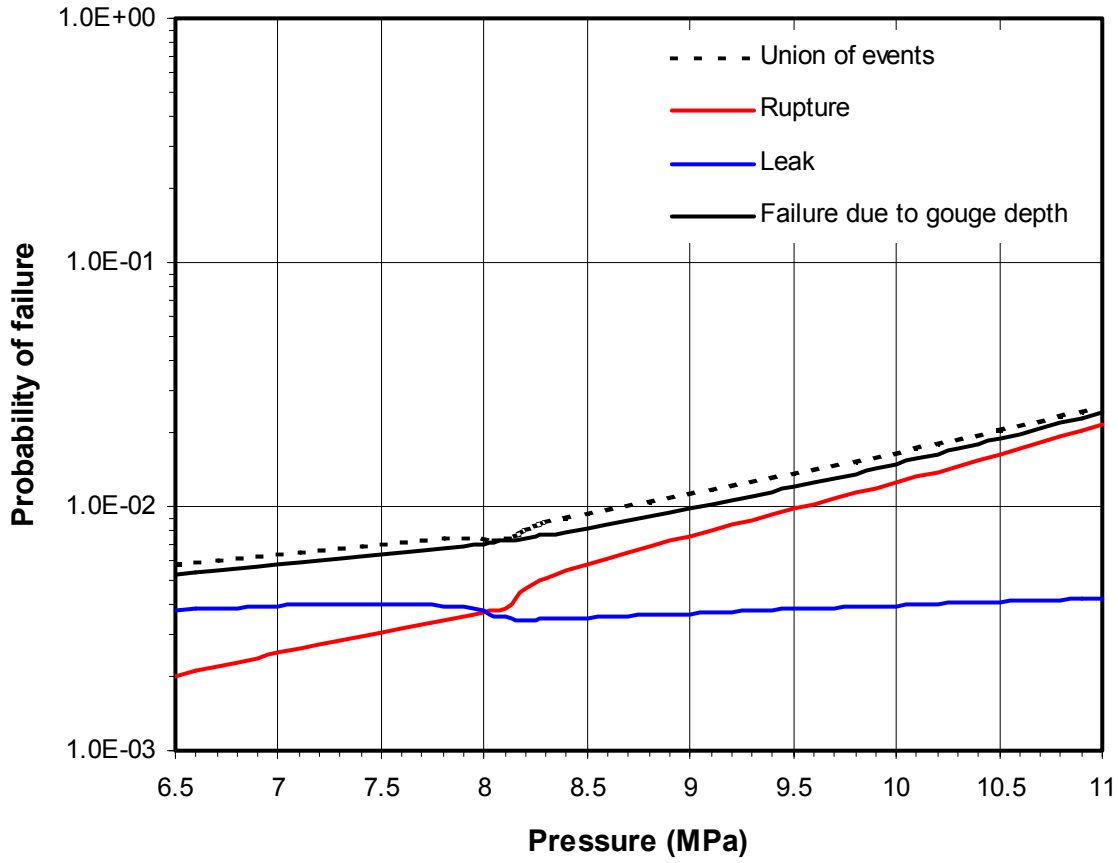

Figure 3.7 FORM results for leak, rupture and loss of containment

3.3 ANOMALY IN SORM RESULTS

With first-order reliability methods approximating the failure surface by a hyperplane becomes less accurate as the failure surface becomes more curved. Thus, it may be expected that the curvature of the failure surface could be used to approximate the failure surface with a better or more accurate surface for which the probability content can be evaluated exactly. A number of approaches have been proposed and used. These are generally based on fitting a parabolic, quadratic or higher-order surface to the actual surface at the beta-point.

The most common approach is based on asymptotic concepts put forward by Laplace in 1821 and developed by Breitung [4], and uses:

$$P_f \approx \Phi(-\beta)\prod_{i=1}^{n-1}(1-\beta\kappa_i)^{1/2}$$

where $\kappa_i = -\left[\frac{\partial^2 y_n}{\partial y_i^{\,2}}\right]$ is the i^{th} principal curvature of the failure surface at the beta-point.

The error in the asymptotic approximation is unknown, but P_f tends to the exact value as $\beta \to \infty$. It is also known that the asymptotic failure estimate improves a first-order estimate if the failure surface is 'almost plane'.

However, it can be seen that the above approximation fails if $\beta\kappa_i > 1$, i.e. if the radius of curvature at the beta-point for one (or more) of the principal variables is greater than β.

In order to consider the anomaly in the second-order reliability results, it is necessary to consider how SORM is formulated in the reliability analysis software used; the proprietary package SYSREL has been used here, but most commercial reliability analysis programs follow a similar approach.

For a single failure function, or surface, the second-order probability of failure is evaluated from:

$$P_{f_{SORM}} = \Phi(-\beta)\prod_{i=1}^{n-1}(1-\beta\kappa_i)^{1/2} = \Phi(-\beta)C_{SORM}$$

The term $\Phi(-\beta)$ is the first-order estimate of the reliability. Thus, the first step of a SORM analysis is to find the beta-point, i.e. the closest point to the origin in U-space. The term C_{SORM} may be considered as a correction on the first-order reliability estimate. Generally, this correction term is close to one.

In essence, this second-order reliability method is based on approximating the failure surface by a paraboloid through the beta-point in U-space.

The main curvatures are found from the Hessian matrix of second derivatives of the failure function. Thus, the failure surface must be continuous and twice differentiable, at least at the beta-point.

To evaluate a second-order estimate of the probability of the intersection of two or more events, a similar approach is followed in which a correction term is applied to the first-order results.

Initially, it was suggested that the anomaly observed in the SORM results for this example may be due to a discontinuity in the failure surface. However, by plotting out the failure surface it can be shown that is not the case. It has also been suggested that the problem may arise because of the evaluation of the intersection for the two failure events. Whilst this may contribute to the problem, it is not the main cause, as is shown below by considering only one failure event (i.e. the failure function for gouge depth).

In the following sub-sections the failure surface and SORM results are considered at pressures either side of the anomaly, i.e. pressures of 7.0 MPa and 9.0 MPa, and at the pressure (or close to the pressure) where the anomaly occurs, i.e. 8.15 MPa.

3.3.1.1 Results at 7.0 MPa

Since in the case study example only two basic variables are involved in the reliability analysis, the failure surface can be plotted in two dimensions. Figure 3.8 is a plot of the failure surface in U-space at a pressure of 7 MPa.

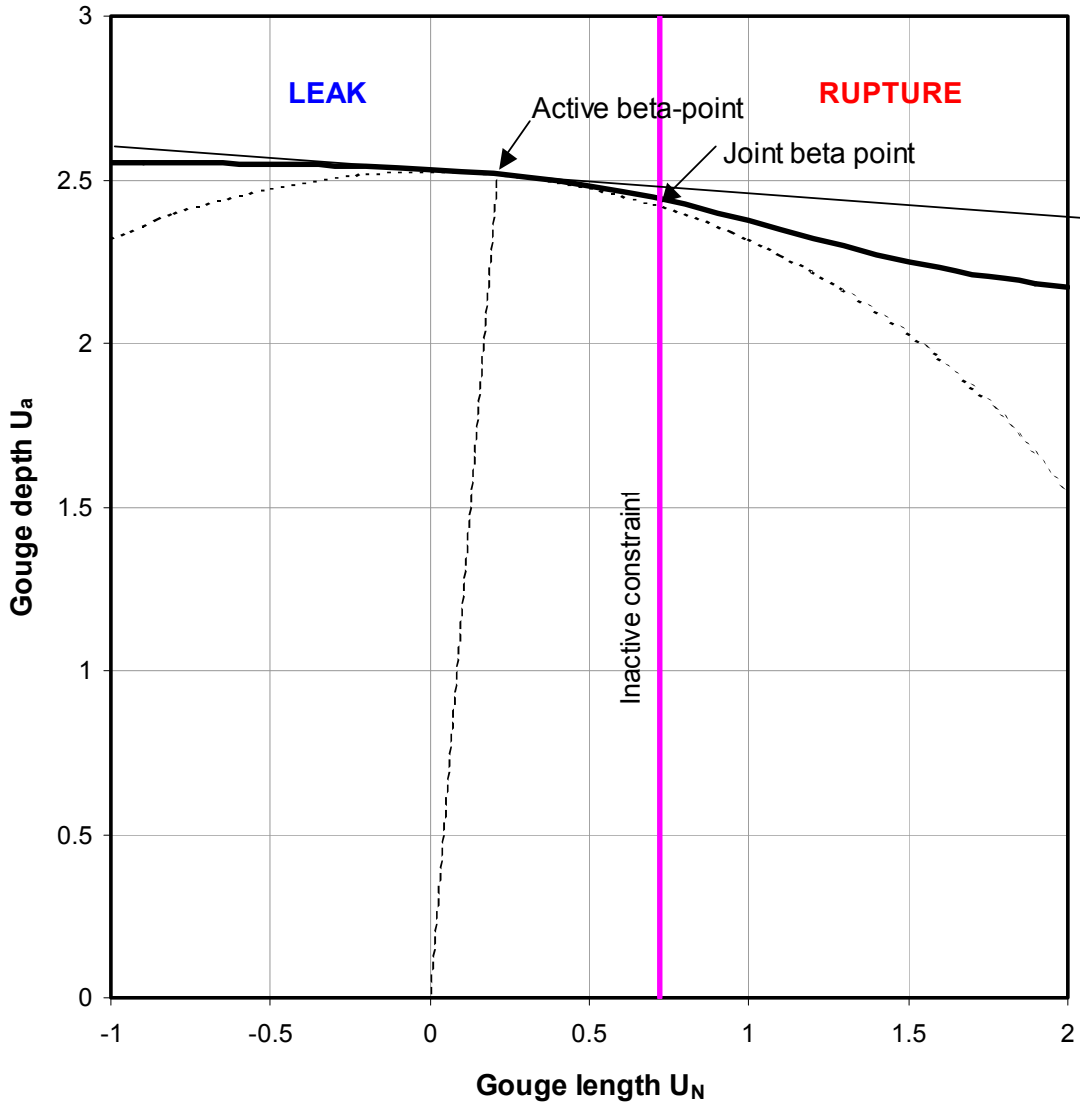

Figure 3.8 U-space plot of case study results at a pressure of 7 MPa

The failure surface for gouge depth is shown as a solid heavy black line, and the failure surface for gouge length is shown as a solid purple line. The critical gouge length is not a function of gouge depth, and is therefore parallel to the gouge depth axis. The joint beta-point, where the two failure surfaces intersect, is depicted on the figure.

The total region outside the gouge depth failure surface defines the failure region for loss of containment; this region to the left of the gouge length failure surface defines the failure region

governed by a leak, and to the right of the gouge length failure surface defines the failure region governed by a rupture.

The closest point to the origin is also shown, and this is the active beta-point to evaluate the probability of failure for a leak; the gouge depth failure surface is active, and the gouge length failure surface is an inactive constraint. The joint-beta point is the closest point to the origin for the rupture region. It is clear that at a pressure of 7.0 MPa failure is most likely to occur through a leak.

Also shown is a tangent or hyperplane at the beta-point. A circle or hypersphere of radius β through the beta-point is shown by a dashed line.

Since the gouge depth failure surface is concave at the beta-point when viewed from the origin, the first-order estimate of the failure probability for loss of containment will underestimate the 'true' failure probability. A second-order estimate accounts for the curvature of the failure surface at the beta-point and introduce a correction term; SYSREL gives a value of C_{SORM} of 1.47 at this pressure. The first-order estimate for probability of failure is 5.78×10^{-3} ($\beta = 2.52$), thus the second-order estimate is $(5.78 \times 10^{-3}) \times 1.47 = 8.49 \times 10^{-3}$ (equivalent $\beta = 2.39$). Monte Carlo simulation using an adaptive technique and enough trials to converge to the exact failure probability obtained 6.55×10^{-3} (equivalent $\beta = 2.48$). Thus, in this case FORM gives a better estimate to the 'true' failure probability than SORM. The results are summarised in Table 3.1.

	FORM	**C_{SORM}**	**SORM**	**Monte Carlo**
Loss of containment	5.78×10^{-3} ($\beta = 2.52$)	1.468	8.49×10^{-3} (equivalent $\beta = 2.39$)	6.55×10^{-3} (equivalent $\beta = 2.48$)
Leak	3.91×10^{-3} ($\beta = 2.66$)	1.468	5.74×10^{-3} (equivalent $\beta = 2.53$)	4.19×10^{-3} (equivalent $\beta = 2.64$)
Rupture	2.50×10^{-3} ($\beta = 2.81$)	1.00	2.50×10^{-3} (equivalent $\beta = 2.81$)	2.35×10^{-3} (equivalent $\beta = 2.83$)

Table 3.1 Probability of failure results at a pressure of 7 MPa

To evaluate the probability of a leak, the inactive constraint can be considered, and the first-order probability estimated as 3.91×10^{-3} ($\beta = 2.66$). For the second-order estimate, C_{SORM} is again around 1.47, and the second-order probability of a leak is $(3.91 \times 10^{-3}) \times 1.47 = 5.74 \times 10^{-3}$ (equivalent $\beta = 2.53$). Again, from comparison with the Monte Carlo results shown in Table 3.1 FORM gives a better estimate to the 'true' failure probability than SORM.

To evaluate the probability of a rupture, the probability of intersection of the two failure surfaces needs to be considered and the joint beta-point found. The first-order probability estimated as 2.50×10^{-3} ($\beta = 2.81$). However, it can be seen that at the joint beta-point the gouge depth failure surface is, or is close to, a point of inflection. The curvatures of the two failure surfaces at the joint beta-point are small, and this is shown by the second-order correction term C_{SORM} which is evaluated as 1.00. Thus the FORM and SORM results are identical.

3.3.1.2 Results at 9.0 MPa

Figure 3.9 shows a corresponding plot for results at a pressure of 9.0 MPa, which is a pressure well in excess of the pressure where the anomaly occurs.

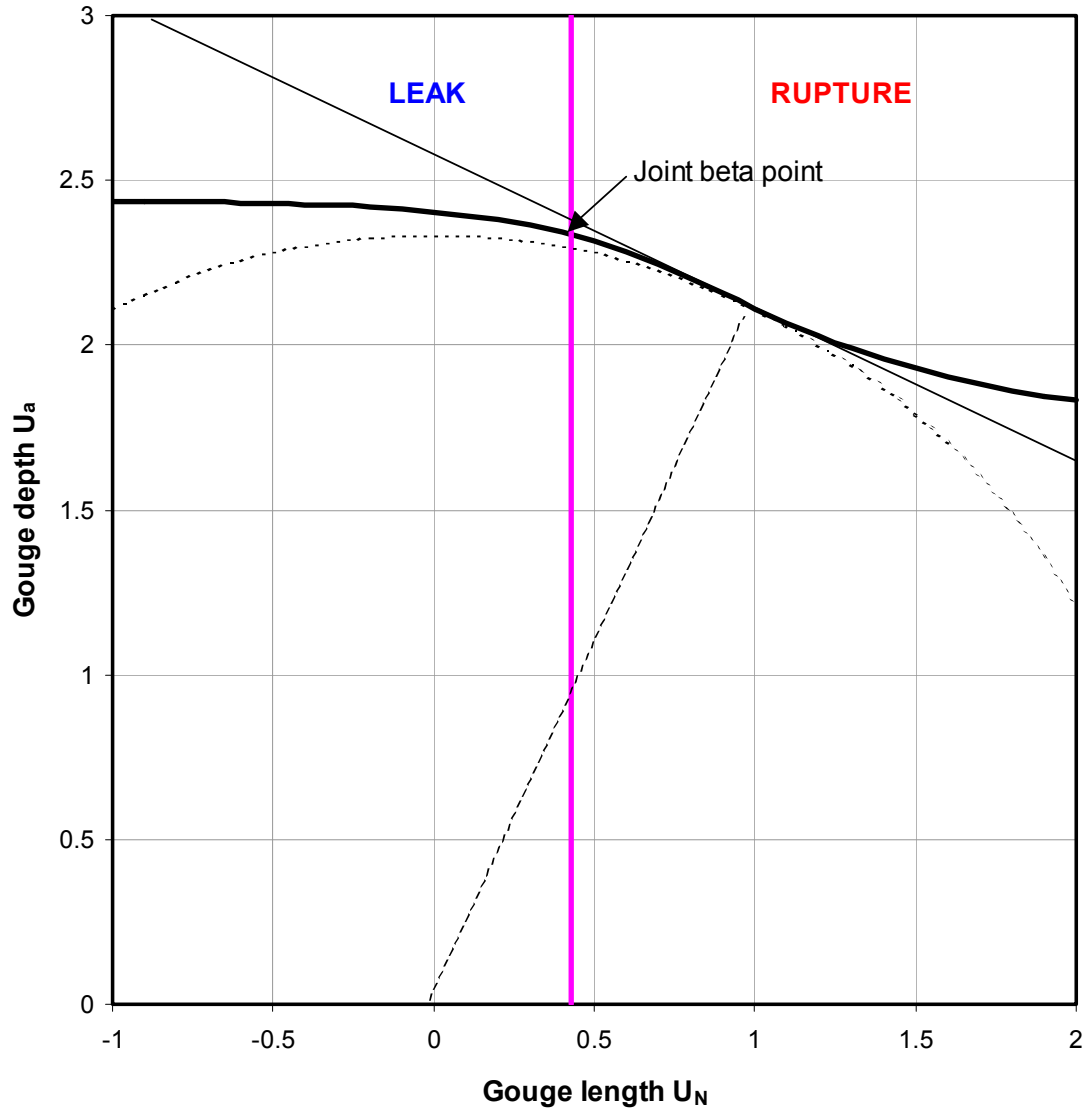

Figure 3.9 U-space plot of case study results at a pressure of 9 MPa

The closest point to the origin is the active beta-point to evaluate the probability of failure for a rupture, and it is clear that at this pressure rupture is the most likely failure mode. The figure suggests that the curvatures of the failure surface are small at the beta-point. However, there is

some local curvature which is convex when viewed from the origin, and the SORM correction term is 0.844. It is clear from the figure that at a larger scale the surface is not convex, but appears to be a point of inflection at or near the beta-point, and this is also shown by the Monte Carlo result which is near to the FORM estimate.

The probability of a leak is evaluated using the joint beta-point; at this point the curvatures of the two failure surfaces are small, and this is shown by the second-order correction term C_{SORM} which is evaluated as 1.00.

The first-and second-order probability results are given in Table 3.2.

	FORM	**C_{SORM}**	**SORM**	**Monte Carlo**
Loss of containment	9.77×10^{-3} ($\beta = 2.33$)	0.844	8.24×10^{-3} (equivalent $\beta = 2.40$)	11.1×10^{-3} (equivalent $\beta = 2.29$)
Leak	3.64×10^{-3} ($\beta = 2.68$)	1.00	3.64×10^{-3} (equivalent $\beta = 2.68$)	5.11×10^{-3} (equivalent $\beta = 2.57$)
Rupture	7.57×10^{-3} ($\beta = 2.43$)	0.844	6.39×10^{-3} (equivalent $\beta = 2.49$)	6.65×10^{-3} (equivalent $\beta = 2.48$)

Table 3.2 Probability of failure results at a pressure of 9 MPa

3.3.1.3 Results at 8.15 MPa

Figure 3.10 shows a plot of the results evaluated at a pressure of 8.15MPa, which is the pressure at or near to where the step in the probability for the failure modes occurs in this case.

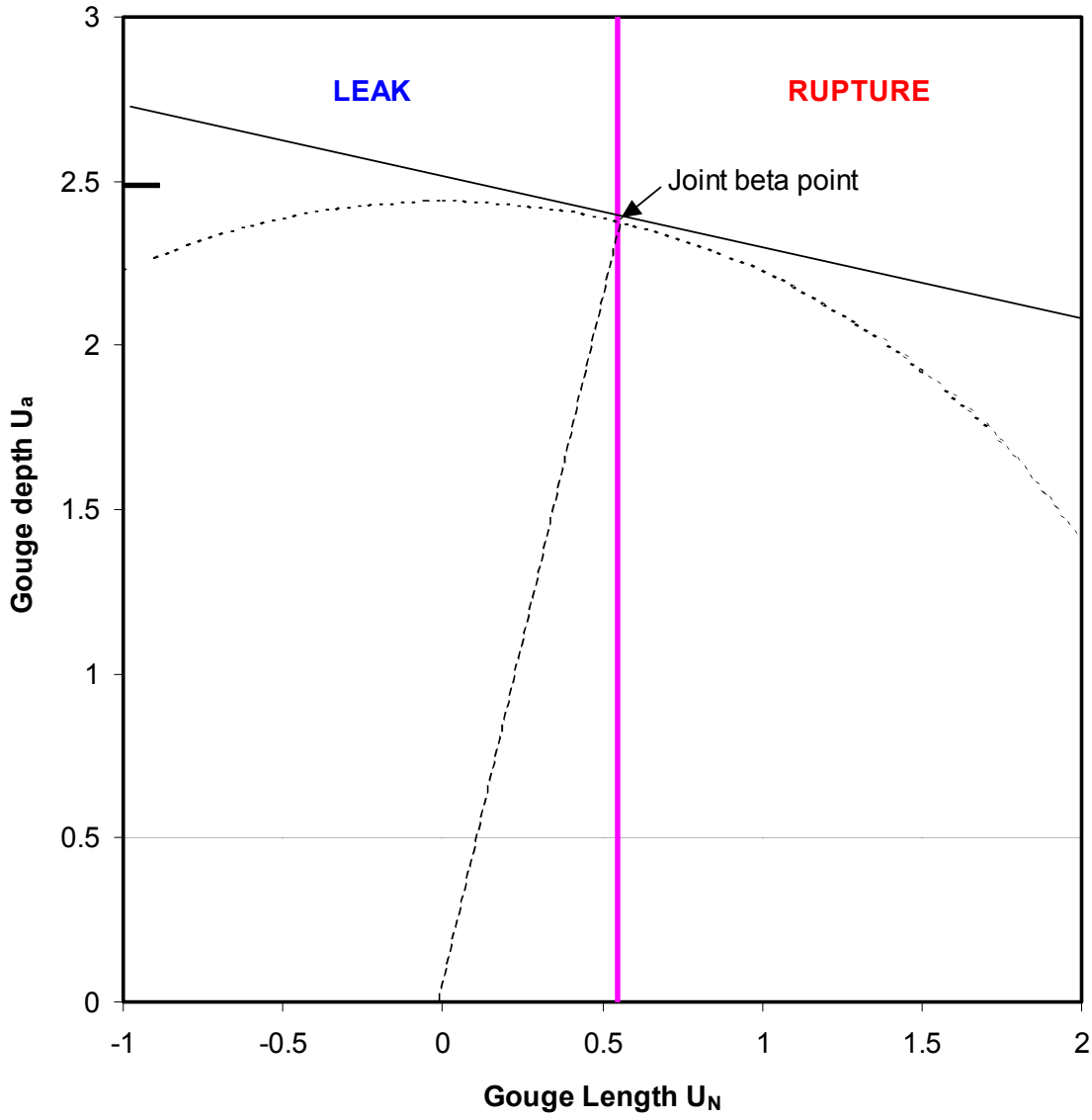

Figure 3.10 U-space plot of case study results at a pressure of 8.15 MPa

The closest point to the origin is also the joint beta-point. It can be seen that at the beta-point the failure surface follows the surface of a hypersphere very closely. This causes a number of problems.

Firstly, it is very difficult for the first-order reliability analysis to converge to the beta-point because the distance to the origin is equal or very similar over a significant area of the failure surface.

Secondly, and perhaps most importantly, it causes problems with SORM analysis. At this pressure the curvatures of the failure surface are such that a paraboloid cannot be fitted. The schematic

illustration in Figure 3.11 shows the problem for a reliability index of 3.0. The figure shows the hyperplane or tangent at the beta point, a hypersphere of radius 3.0, and a paraboloid fitted at the beta point. Clearly, if the failure surface is such that it approximates a hypersphere in the vicinity of the beta-point the curvature of the surface is such that it is not possible to fit a paraboloid to it.

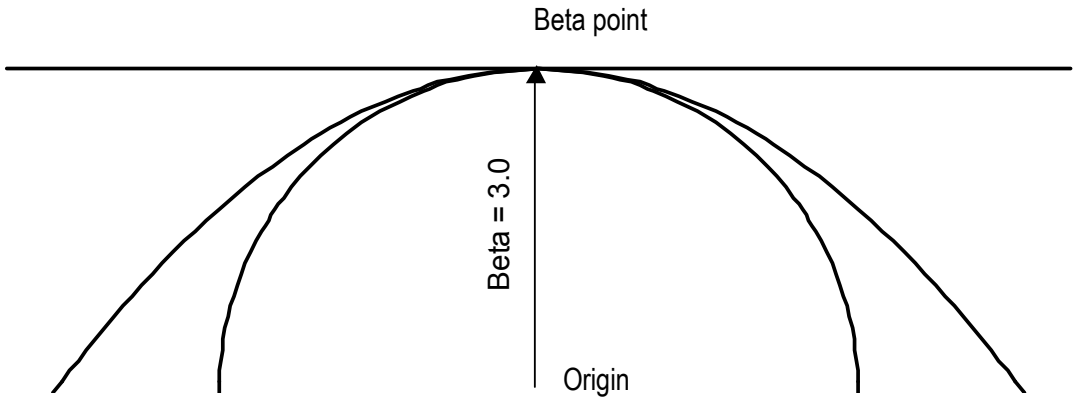

Figure 3.11 Illustration of curvatures at the beta-point

It is of course possible to fit an alternative second-order function, or higher-order function to the surface, however such functions are not amenable for use in general-purpose software. A paraboloid has theoretical justification, which is not the case for alternative functions. Unforunately, the use of a paraboloid has limitations, as the present example shows.

Another effect of the very significant curvatures is that the SORM correction term becomes large, and when it becomes very large, such that a paraboloid cannot be fitted, SYSREL defaults to the FORM solution. This can be investigated by looking at the SORM correction term at pressures either side.

A plot of the SORM correction term versus pressure is shown in Figure 3.12. Close to a pressure of 8.15 MPa values of the correction term in excess of 25 were evaluated. Below a pressure of around 8.6 MPa the SORM correction term is greater than one, which means that the failure surface is concave at the beta-point when viewed from the origin.

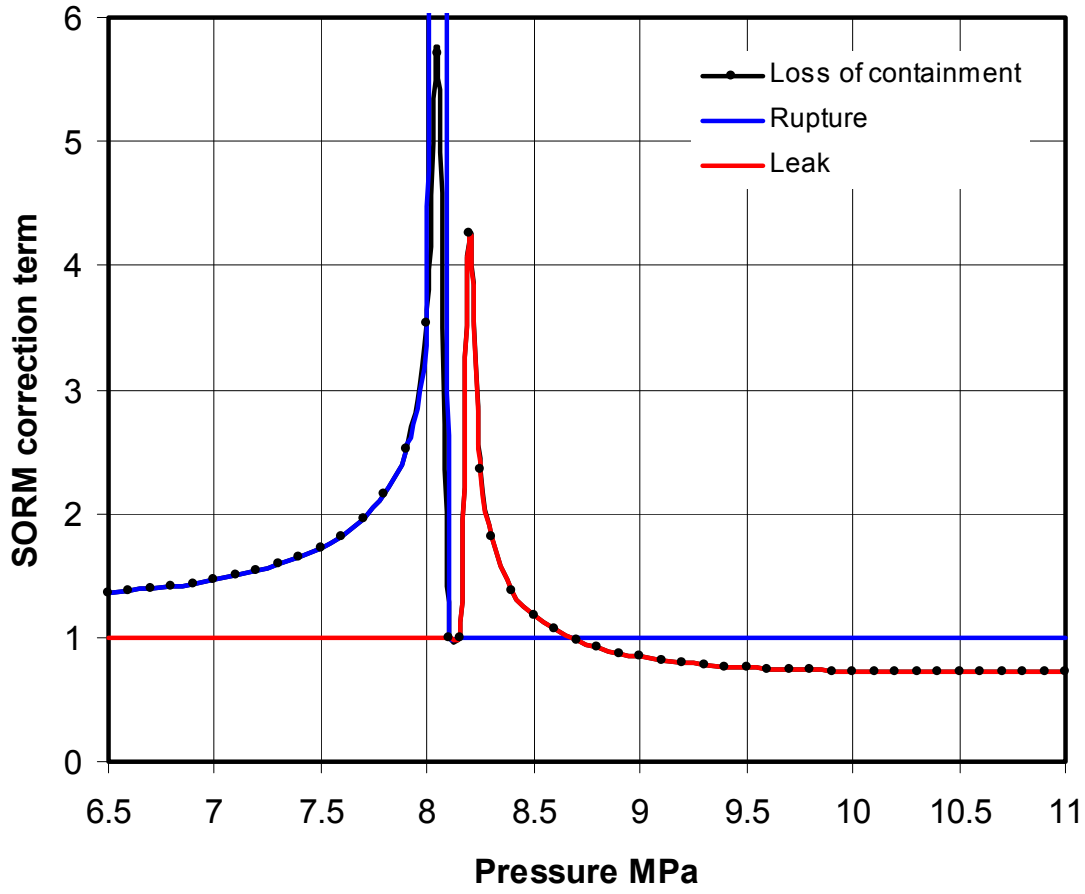

Figure 3.12 SORM correction term

The first-and second-order probability results are given in Table 3.3, along with the results from Monte Carlo analysis.

	FORM	C_{SORM}	SORM	Monte Carlo
Loss of containment	7.29×10^{-3} ($\beta = 2.44$)	Error	7.29×10^{-3} (equivalent $\beta = 2.44$)	8.76×10^{-3} (equivalent $\beta = 2.38$)
Leak	3.40×10^{-3} ($\beta = 2.71$)	Error	3.40×10^{-3} (equivalent $\beta = 2.71$)	4.77×10^{-3} (equivalent $\beta = 2.59$)
Rupture	4.20×10^{-3} ($\beta = 2.64$)	Error	4.20×10^{-3} (equivalent $\beta = 2.64$)	4.23×10^{-3} (equivalent $\beta = 2.63$)

Table 3.3 Probability of failure results at a pressure of 8.15 MPa

Plots of the reliability results for FORM, SORM and Monte Carlo results at selected pressures are shown in Figures 3.13, 3.14, and 3.15 for leak, rupture, and loss of containment (defined by the gouge depth criterion only) respectively. From the Monte Carlo results it is clear that the SORM estimates around a pressure of 8.15 MPa are in error.

Since Figure 3.15 is based on one failure function only, i.e. for gouge depth, it is clear that the anomaly in the SORM results is primarily due to the curvature of one failure surface, and is not due to the intersection of two events.

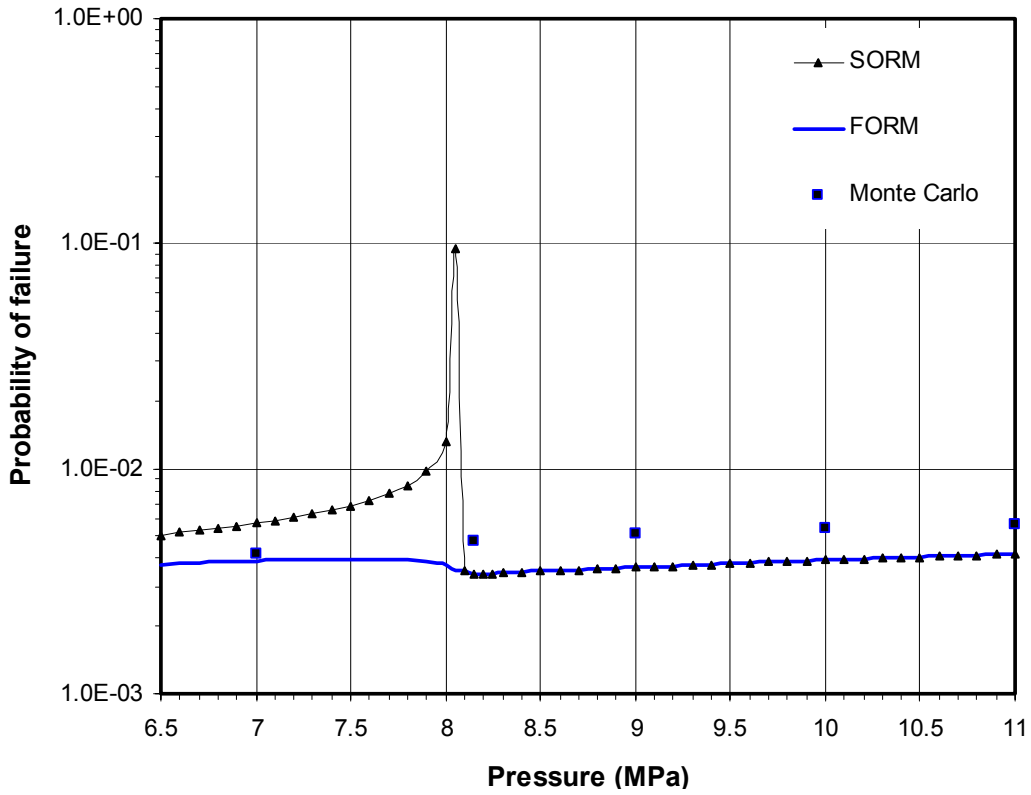

Figure 3.13 Probability results for Leak

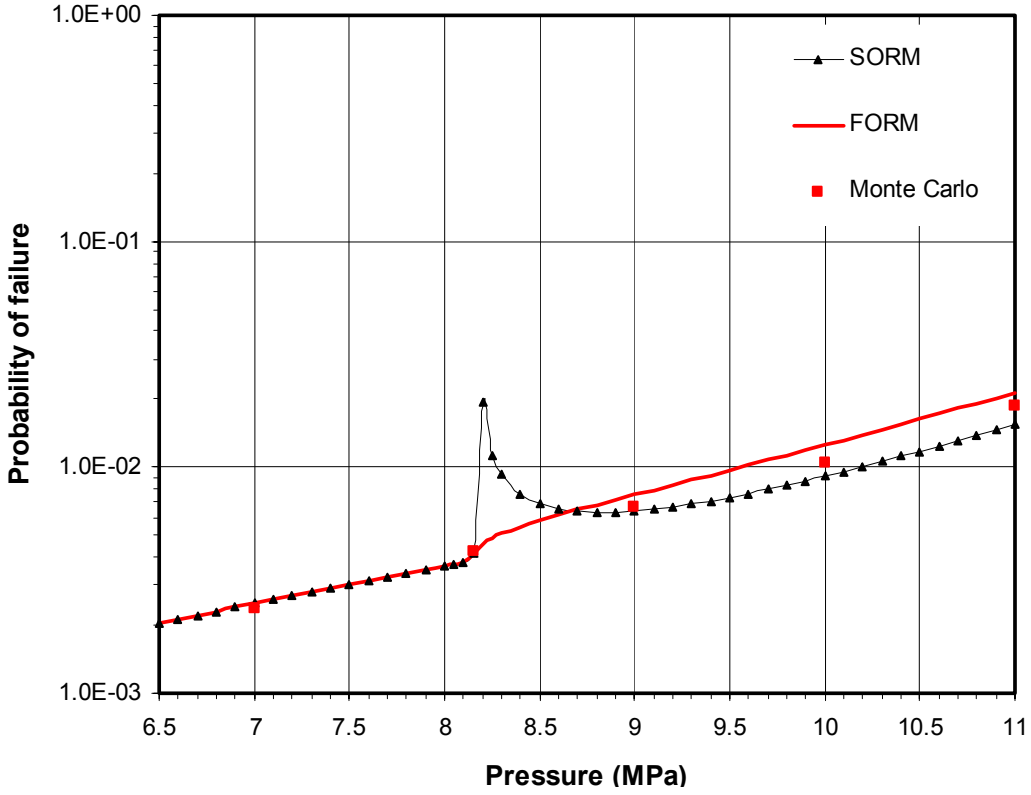

Figure 3.14 Probability results for Rupture

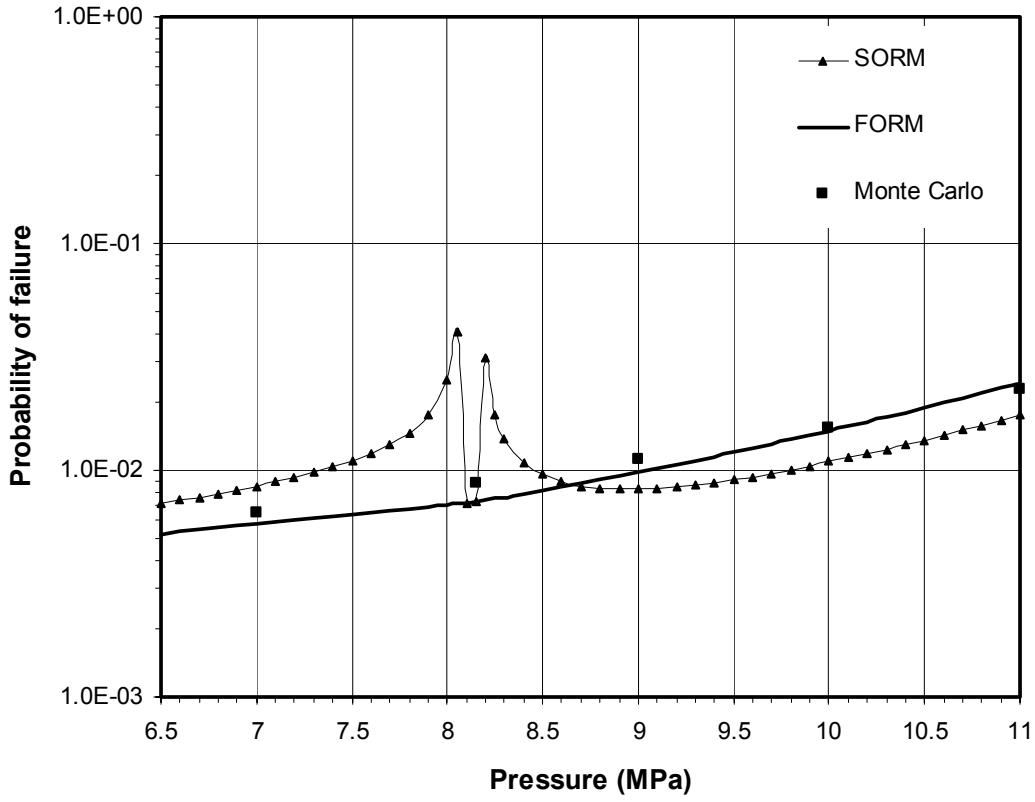

Figure 3.15 Probability results for loss of containment

4. CONCLUSIONS

4.1 PREAMBLE

BG, in the original work, used direct integration to compute probabilities of failure. Results at only two pressures (around 7 and 9 MPa) are presented in the BG report, and they indicate that failure is governed by leak at both pressures.

Independent analysis by BOMEL in a case study for a Competition of Ideas project using first- and second-order reliability methods indicated that the governing mode switched from leak to rupture at the higher pressure. However, investigating the failure probability over a range of pressures highlighted numerical anomalies that were completely unexpected. These were:

- A step in evaluated probabilities and a change in the governing failure mode from leak to rupture at, or near, the same pressure.
- A 'spike' in probabilities evaluated using the second-order reliability method (SORM) at an interim pressure. Because SORM analysis accounts for the curvature of the failure surface, it usually gives a more accurate answer than first-order linear methods.

To investigate these anomalies the original problem has been simplified. Only two random variables have been used, but the essential elements of the problem, trends in failure probabilities, etc, and the anomalies have been retained.

4.2 NUMERICAL ANOMALIES

4.2.1 Step in reliability results

The change in governing failure mode from leak to rupture at around a pressure of 8.15 MPa has been confirmed, and is due to the particular modelling and probability distributions used. The exact value of the switchover in governing failure modes depends on the particular numerics of the problem, and to some extent on the reliability analysis method used.

The jumps in the first-order estimates of failure probabilities that were evaluated in the case study have been shown to be as a result of using a default option in the SYSREL program to switch off the evaluation of probabilities associated with inactive constraints. By including evaluation of the inactive constraints better first-order estimates of the failure probability are evaluated. It is the default in SYSREL to switch off the inactive constraints because it is not usually necessary, and because of the increased numerical effort which can be significant for complex problems.

4.2.2 Numerical anomaly in SORM results

The SORM results show that there appears to be a "hotspot" where probabilities of failure rise extremely rapidly, possibly leading to unacceptable high values within a "spike" of probability.

The reasons for the presence of this hotspot in the SORM results is a highly curved region of the failure surface, that sits close to the origin in basic variable space and exists under certain combinations of variables.

The Monte Carlo results do not exhibit a spike in probability, and are similar to the FORM results. This is comforting and confirms that the problem is with the numerics of SORM, rather than the behaviour of the mathematical functions used to describe the mechanism, or worse some physical attribute or instability of real pipes that occurs at specific pressures.

In a great many cases of reliability analyses the differences between failure probabilities predicted using FORM and SORM will be small. Nevertheless, it is advisable in any problem to confirm this – or otherwise – by performing both types of analyses. SORM estimates are often more accurate because they include more information about the failure surface. However for practical cases, FORM analysis usually provides sufficiently accurate estimates of failure probability.

4.3 CONCLUSIONS

This investigation into the anomalies has shown that the evaluated reliabilities are partly as a result of the particular modelling and probability distributions used in the problem, and partly as a result of the application of the reliability analysis methodology used; the anomalies are not as a result of a "real" aberration in pipeline behaviour under pressure.

The particular circumstances that have lead to the anomaly in the SORM results, whilst interesting, are believed to be unusual in practice. The particular failure function and probability distribution modelling lead to circumstances where the standard second-order reliability methods usually used in general-purpose software breakdown. In this case, it is evidenced by the very large second-order correction terms that are applied to the FORM results at particular pressures.

The case study analysis was undertaken using commercial reliability software, and this work has shown that when undertaking reliability analysis of even a simple problem it is very important to have a thorough understanding of the theory, the software, convergence tolerances, and the various analysis options available.

This investigation has also shown that when undertaking a reliability analysis of this sort it is important to undertake parameter studies, sensitivity studies, and to check the evaluation of the failure probability using at least two alternative methods. These points were recommended in the final report for the Competition for Ideas project [1].

5. REFERENCES

1. BOMEL. 'Probabilistic methods: uses and abuses in structural integrity. BOMEL report C891\04\032R Rev A, September 2001.

2. Edwards A M, Espiner R J & Francis A. 'Example of the application of limit state, reliability and risk based design to the uprating of an onshore pipeline'. BG Technology Report No. R3125, Issue No 2, 6 September 1999.

3. R C P Consult. 'COMREL and SYSREL Users Manual', RCP GmbH, Barer Strasse 48/111, 80799, München, 1996.

4. Breitung K. 'Asympotic approximation for multinormal integrals', J. Eng. Mech., ASCE, Vol. 110, No. 3, 1984.

Printed and published by the Health and Safety Executive
C1.25 10/02

MAIL ORDER
HSE priced and free
publications are
available from:
HSE Books
PO Box 1999
Sudbury
Suffolk CO10 2WA
Tel: 01787 881165
Fax: 01787 313995
Website: www.hsebooks.co.uk

RETAIL
HSE priced publications
are available from booksellers

HEALTH AND SAFETY INFORMATION
HSE InfoLine
Tel: 08701 545500
Fax: 02920 859260
e-mail: hseinformationservices@natbrit.com
or write to:
HSE Information Services
Caerphilly Business Park
Caerphilly CF83 3GG

HSE website: www.hse.gov.uk

RR 021

£10.00

ISBN 0-7176-2574-5

9 780717 625741